ChemComm

Enzyme-Regulated Topology of a Cyclic Peptide Brush Polymer for Tuning Assembly

Journal:	*ChemComm*
Manuscript ID	CC-COM-07-2015-005653.R1
Article Type:	Communication
Date Submitted by the Author:	12-Sep-2015
Complete List of Authors:	Wang, Zhao; UCSD, Li, Yiwen; UCSD, Huang, Yuran; UCSD, Thompson, Matthew; University of California, San Diego, LeGuyader, Clare; University of California, San Diego, Sahu, Swagat; University of California, San Diego, Gianneschi, Nathan; University of California, San Diego, Chemistry & Biochemistry

Journal Name

COMMUNICATION

Enzyme-Regulated Topology of a Cyclic Peptide Brush Polymer for Tuning Assembly

Received 00th January 20xx,
Accepted 00th January 20xx

DOI: 10.1039/x0xx00000x

www.rsc.org/

Zhao Wang,[a‡] Yiwen Li,[a‡] Yuran Huang,[a, b] Matthew P. Thompson,[a] Clare L. M. LeGuyader,[a] Swagat Sahu[a] and Nathan C. Gianneschi*[a,b]

Norbornenyl cyclic elastin-like peptides were polymerized *via* ring opening metathesis polymerization (ROMP) to generate thermally responsive brush polymers. The thermally-responsive nature of the materials could be attenuated by the addition of a proteolytic enzyme that causes the cyclic peptide side chains to be linearized.

Responsive polymers undergo changes in properties triggered by a single stimulus, or multiple stimuli, including temperature,[1] pH,[2] light,[3] magnetic fields[4] and enzymatic activity.[5] These polymers represent a growing class of smart materials that are finding an increasingly important role in various applications, such as drug delivery,[6, 7] tissue engineering,[8] and biosensing.[9] The incorporation of enzyme responsive elements into polymers is particularly intriguing since enzymes show high substrate specificity, operate under biologically relevant conditions, and may prove useful in sophisticated tissue targeting applications.[10-13] While the majority of polymer-peptide bioconjugate systems to date have involved graft-onto conjugation reactions,[14] graft-from polymerization[15] or graft-through polymerization[16] to generate brush polymers of linear peptides, we have become interested in incorporating cyclic peptides. This work is motivated by the fact that cyclic structures can possess unusual macroscopic properties not observed for the analogous linear form of the same sequence. As such, they have been employed in self-assembled nanostructures,[17, 18] as ligands for cellular receptors (e.g. RGD, antibiotics),[19] and for proteolytic resistance.[20]

We utilized a well-known thermally responsive peptide, constrained in its cyclic form, wherein enzymatic action would provide a switch from a cyclic sequence to a linear one, resulting in dual responsive polymers and polymeric micellar nanoparticles. As a demonstration of this concept, we chose to focus on elastin-like polypeptides (ELPs) as thermally responsive and enzymatically triggerable elements when displayed as brush side-chains on a polynorbornene backbone. The most commonly used ELPs are composed of multiple repeat units of the peptide sequence $(VPGXG)_n$, where X can be any amino acid other than proline.[21] The preparation of polymeric forms of ELPs has been previously achieved by recombinant methods or *via* polymerization of monomers with short elastin sequences.[22, 23] In contrast, the exploration of ELPs with unconventional, nonlinear topologies has been limited to the work of Tirrell and co-workers, in which a series of ELPs of circular, tadpole, star, and H-shape were prepared by genetically encoded SpyTag–SpyCatcher chemistry.[24] While this work constituted a thorough study of non-linear ELPs, these materials were not fully explored for their stimuli-responsive behaviour.

We began by polymerizing cyclic norbornenyl-ELP monomer **1** (Fig. 1). The behaviour of the resulting polymer was explored with and without enzymatically treating the material to generate the linearized polymeric side-chain. We note, the synthetic scheme included the addition of a novel, functional gadolinium-DOTA based termination agent (**Gd-TA**, Fig. 1), to provide a tag for magnetic resonance imaging (MRI) in future applications of these materials as *in vivo* imaging agents.[25] We believe it is prudent to include labels and tags of this kind early in the development of materials, and the termination chemistry proves a robust way to achieve this. [26]

We hypothesized that the cyclic ELP-polymer would result in a decreased lower critical solution temperature (LCST) with respect to the enzymatically linearized version of the ELP-polymer sidechains. This idea was predicated on the fact that cyclic peptides are inherently more hydrophobic (no terminal amines and carboxylic acids) when compared to the linear analogue, and they consist of a repeated ELP unit in the form of $(VPGXG)_2$ not present in the linear sequence.[22, 27]

Norbornene monomer **1** contains an elastin-based sequence VPGGGVPGLG (Fig. S1), with an added lysine moiety to allow for the cyclization reaction, and a norbornenyl moiety (Nor-Gly) (See ESI†) to provide a handle for ring opening metathesis (ROMP). The cyclization reaction was performed using standard solid phase peptide synthesis (SPPS) methods with a longer reaction time (5

[a] *Department of Chemistry and Biochemistry, University of California, San Diego, 9500 Gilman Dr., La Jolla, CA 92093, USA. Email: ngianneschi@ucsd.edu*
[b] *Materials Science and Engineering, University of California, San Diego, 9500 Gilman Dr., La Jolla, CA 92093, USA.*
† Electronic Supplementary Information (ESI) available: Experimental details and additional information. See DOI: 10.1039/x0xx00000x
‡ These authors contributed equally to this work.

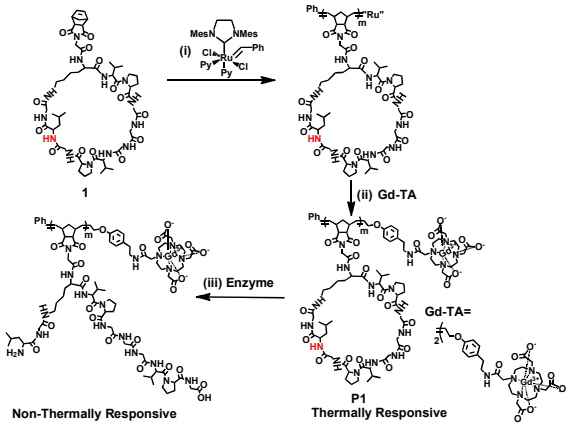

Fig. 1. Synthetic scheme of hompolymer **P1** using ROMP initiator $(IMesH_2)(C_5H_5N)_2(Cl)_2Ru$=CHPh ("Ru") and Gd-containing termination agent (**Gd-TA**). For **P1**, m = 5. The structure post-enzyme treatment is drawn to represent the ideal result of 100% peptide cleavage. Enzyme cleavage site is shown in red color.

days) and at lower concentration (1 mg/ml) to avoid intermolecular coupling (See ESI†).[28] Compound 1 was purified by preparative scale high-performance liquid chromatography (Prep-HPLC) with the structure and purity confirmed by electrospray ionization mass spectrometry (ESI-MS) and analytical HPLC (Fig. S2).

Thermolysin was used to interrogate the effect of enzyme activity on the topology of ELP-polymers. The enzyme is a thermostable Zn-metalloprotease that cleaves at the N-terminus of hydrophobic residues (Ile, Leu, Val, Ala, Met, Phe) flanked by proline[29] (along the C-terminal direction). In this work, it serves as a model enzyme to investigate the enzyme-responsiveness of the ELP-polymers. To study enzymatic action, we designed a sequence with a single cleavage site (only position 1 of **1** can be cleaved by thermolysin) (Fig. S9), so that the amino acid residues would remain bound to the polymer after enzymatic cleavage. This results in the formation of a Y-shape linear peptide without generating a truncated peptide by-product. We confirmed this by incubating **1** with thermolysin. HPLC analysis shows 100% cleavage in less than 1 h upon treatment with thermolysin, while treatment of **1** with denatured enzyme showed no cleavage by HPLC (Fig. S10). Product masses were all confirmed by ESI-MS analysis (Fig. S11).

Homopolymer **P1** was prepared via ROMP[30] using a modified 2nd generation Grubbs' catalyst[31] (Fig. 1) followed by termination with **Gd-TA**. Excess termination agent was removed during dialysis, as confirmed by HPLC (Fig. S12). The purified polymer **P1** was characterized by HPLC, MALDI-TOF mass spectrum (MS) and size exclusion chromatography coupled with a multiangle light scattering detector (SEC-MALS). In the MALDI-TOF MS (Fig. 2), the average molecular weights of the peaks match well with the calculated values (*e.g.,* for 5-mer, observed *m/z* 6409.8 Da *vs.* calcd. 6402.9Da). The SEC trace shows a single peak with a narrow distribution indicating a well-defined polymer with molecular weight of 7000Da and a dispersity of 1.03. These results are consistent with the initial reaction conditions: ([monomer]/[catalyst]) ratio=5:1.)

The LCST of **P1** is similar to many other thermo-responsive

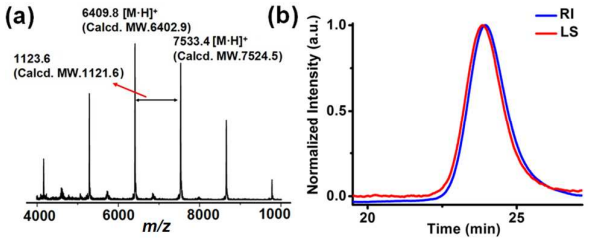

Fig. 2 (a): MALDI-TOF mass spectrum, and (b) SEC trace of **P1**.

polymers, which is greatly affected by molecular parameter (molecular weight, concentration, *etc.*) and environmental parameters (pH, salt concentration and so on).[32] We chose a low degree of polymerization (m = 5) and slightly acidic pH (phosphate buffered saline (PBS) at pH 6) to obtain an LCST near body temperature and to have enzymes retain their activity. The temperature transitions were measured by UV-Vis spectroscopy (Figure 3). The LCST of **P1** is inversely correlated to the solution concentration. That is, the LCST increases from 34 °C to 55 °C as the polymer concentration decreases from 0.6 mg/ml to 0.1 mg/ml respectively. Over this concentration range, the temperature was logarithmic with respect to concentration (Fig. S13). A similar dependence on concentration has also been observed with ELPs synthesized by recombinant protein expression[33] and with synthetic polymers containing short ELP sequences as side chains.[23, 34] It is known that above the LCST, thermo-responsive polymers start to dehydrate and generally self-organize into large amorphous aggregates or precipitate from aqueous solution altogether.[35] Surprisingly, **P1** is able to form ordered fibril structures upon heating in aqueous solution (0.6mg/ml at 40°C), as observed by transmission electron microscopy (TEM) (Fig. 3b). In addition, the fibril structures were observed at various concentrations ((0.6-0.1) mg/ml). Although the detailed mechanism is unknown, we speculate that the hydrophobicity of the whole macromolecule increases above the LCST, providing a suitable driving force for the fiber formation.[36] Visually, upon cooling to room temperature, the cloudy solution became clear in less than 5 minutes and no aggregated state was observed by TEM, indicating a reversible process.

The enzyme sensitivity of **P1** was further investigated by incubating solutions of **P1** with thermolysin at 55 °C for 1 h. Since enzymatic cleavage does not release peptide fragments from the side chains, quantitative analysis of enzyme cleavage proved difficult. HPLC analysis of the reaction showed a large shift in retention time between the starting polymer **P1** and polymer treated with denatured enzyme (Fig. S14). Increasing the incubation time did not change the retention time further, suggesting maximum cleavage was achieved within one hour. A significant increase in LCST (above the detectable range, implying it is higher than 100 °C) was observed as a consequence of breaking the ring structure (Fig. 3c), while samples treated with denatured enzyme (Fig. 3d) showed no significant increase in LCST. Visually, addition of enzyme to an initially cloudy solution of **P1** at 55 °C resulted in the solution gradually becoming clear with no aggregated state observed by TEM. To establish the kinetics of the enzyme-driven supramolecular disassembly process, the enzymatic reaction was monitored by UV-Vis spectroscopy and dynamic light scattering (DLS). This indicates a fast disassembly process as turbidity strongly decreases upon addition of enzyme to a hot

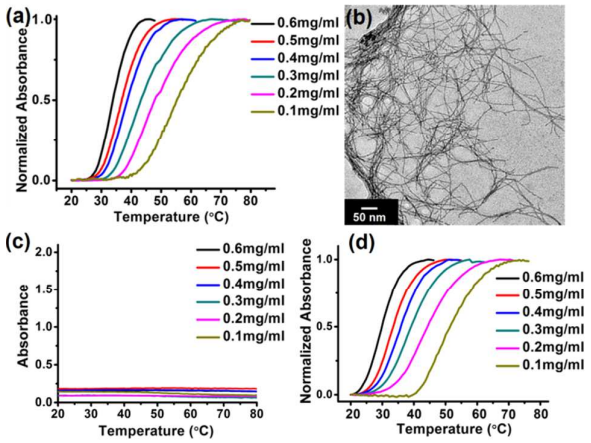

Fig. 3 (a) LCST behavior of **P1** measured by UV-Vis spectroscopy at 550 nm; (b) TEM image of cylindrical structure formed by **P1** (0.6mg/ml) at 40°C. (c) LCST behavior of **P1** treated with thermolysin at 55 °C for 1 h. (d) LCST behavior of **P1** treated with denatured thermolysin at 55 °C for 1 h.

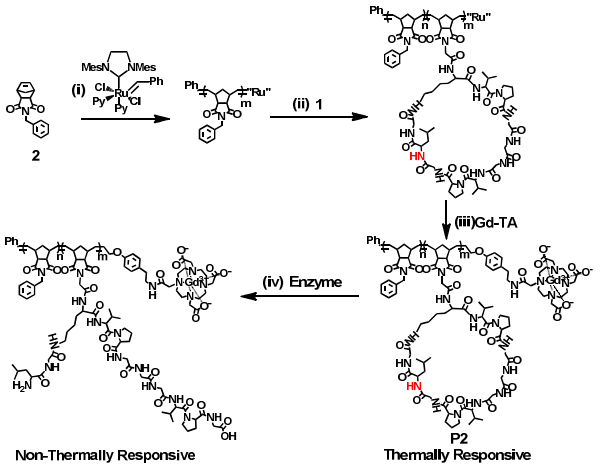

Fig. 4 General synthetic scheme of copolymer **P2** using ROMP initiator "Ru", and **Gd-TA**. For **P2**, m = 5, n = 10. The structure post enzyme treatment is drawn to represent an ideal 100% peptide cleavage. Enzyme cleavage site is shown in red color.

solution (55 °C) of **P1**, whereas untreated **P1** and **P1** treated with denatured enzyme remained in the aggregate state, as shown by only a slight decrease in the absorbance over 1 h (Fig. S15). Similar results were observed by DLS (Fig. S15 (b)) as the scattering intensity of solutions of **P1** significantly drop upon addition of active enzyme compared to the untreated **P1** and **P1** treated with denatured enzyme. Additionally, there was no change in the structure of the fibers in solutions treated with denatured enzyme as observed by TEM (Fig. S16). This enzyme-regulated, switchable thermal behavior is consistent with a linear shaped peptide architecture contributing additional favorable enthalpic interactions with solvent, from the released two chain end groups as well as a decrease in the length of the ELP repeat sequence. That is, enzyme treatment destroys the repeat ELP unit resulting in a linear version that contains only one run of the VPGXG sequence resulting in attenuation of the thermal response.[27]

After observing the thermo- and enzyme-responsiveness of **P1**, we sought to design amphiphilic materials using the cyclic ELP to modulate the hydrophobic/hydrophilic ratio, ultimately allowing us to modulate the morphology of self-assembled micelles.[37] We synthesized a cyclic ELP-based block copolymer by first polymerizing a block of 10 equivalents of norbornenyl-phenyl monomer **2** (Fig. 4), followed by 5 equivalents of monomer **1**. The resulting block copolymer showed narrow and monomodal molecular-weight distribution ($Đ$ = 1.03) (Fig. S17). The number average molecular weight obtained from SEC-MALS (9 kDa) was consistent with the expected degree of polymerization. Spherical micelles with approximately 10 nm in diameter as characterized by TEM and DLS were obtained by adding water to a DMF stock solution containing **P2** (initial concentration: 1 mg/ml) followed by dialysis against water (Fig. 5a and 5d). The LCST of micelles was determined by UV-Vis spectroscopy to be 43 °C (Fig. S18). We postulated that the hydrophilic cyclic ELP corona, that stabilizes the micelle, would become more hydrophobic at elevated temperatures resulting in an aggregation of the micelles due an increase in hydrophobicity. The morphology of the micelles above the LCST was observed by TEM (Fig. 5). The small spherical micelles undergo aggregation to form larger spherical micellar assemblies as determined by TEM and DLS (approximately 20 nm in diameter, Fig. 5b and 5d).[38, 39] The reverse morphology transition, which was achieved by treating the micelles with enzyme, resulted in an increase in the hydrophilicity of the polymer resulting in the morphology shifting back to small spherical micelles (approximately 10 nm, Fig. 5c and 5d). Notably, the morphology could not be completely transferred back to small spherical micelles just by cooling (Fig. S19), probably due to slow kinetics associated with the reorganization of polymer chains with high glass transition temperatures at room temperature.[38] This indicates the significance of the enzyme being required to drive the morphology back to the smaller size. Micelles treated with denatured enzyme show increased size after heating for the same period of time (Fig. S20). The zeta potential shifts towards a more negative value when heated for both the untreated micelles (-20.6 to -26.1 mV) and the denatured enzyme treated micelles (-9.6 to -17.5 mV), suggesting a micellar structural rearrangement occurred (Fig. S21).[40] This is in contrast to the enzyme treated micelles, that remain unchanged when heated, having a zeta potential that remains constant. Finally, the relaxivities of **P1** and **P2** micelles were obtained at a field strength of 7T. Figure S22 shows the relaxivities remained stable after enzyme treatment for both **P1** ((3.0 ± 0.2) $mM^{-1}s^{-1}$ to (3.7 ± 0.4) $mM^{-1}s^{-1}$) and the **P2** micellar nanoparticles ((4.2 ± 0.2) $mM^{-1}s^{-1}$ to (3.4 ± 0.1) $mM^{-1}s^{-1}$). These values are consistent with Gd-DOTA, including macromolecules and nanomaterials observed at 7T field where free rotation at the chelate can occur.[41]

In summary, we have demonstrated that cyclizing a peptide substrate is a unique way of incorporating an enzymatic trigger into a polymeric material. We designed the system based on a strategy predicated on the idea that cyclic peptides and their linear analogues have related but different physical properties resulting from their inherent

Fig. 5 TEM images of **P2** micelles (a) at room temperature, (b) at 55 °C for 6 h, and (c) with enzyme at 55 °C for 6 h. (d) DLS data of

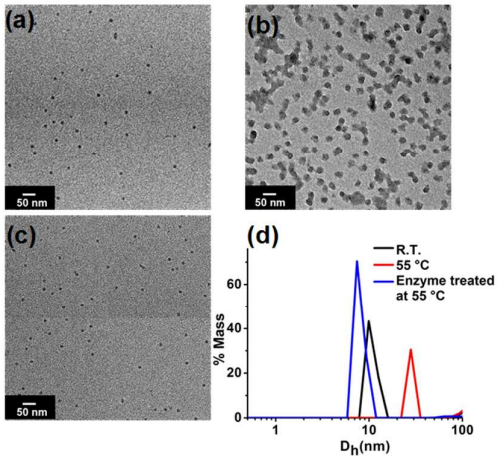

P2 micelles: at room temperature (black curve), at 55 °C for 6 h (red curve), with enzyme at 55 °C for 6 h (blue curve).

topological differences. We anticipate that such an approach may find utility in targeting, followed by programmed clearance and/or retention of related responsive polymeric materials within tissue containing overexpressed enzymes, as is observed for certain metastatic tumors and inflamed tissue. End-labeling polymers with contrast agents may in turn provide a tag allowing tracking of the materials *in vivo* as responsive probes for disease. Ongoing work to develop targeted, thermoresponsive materials, actuated by enzymatic reactions, is underway in our laboratory.

The authors thank generous support of this research from a BRI grant (FA99550-12-1-0414). TEM analysis of materials was conducted at the UCSD Cryo-Electron Microscopy Facility, supported by NIH funding to Dr. Timothy S. Baker and the Agouron Institute gifts to UCSD. We would like to thank the UCSD Molecular MS Facility and University of Akron MS Center for instrumentation. Materia Inc is greatly acknowledged for the donation of catalyst.

Notes and references

1. P. De, S. R. Gondi and B. S. Sumerlin, *Biomacromolecules*, 2008, **9**, 1064-1070.
2. J. Zhang and N. A. Peppas, *Macromolecules*, 2000, **33**, 102-107.
3. F. D. Jochum, L. zur Borg, P. J. Roth and P. Theato, *Macromolecules*, 2009, **42**, 7854-7862.
4. S. D. Kong, W. Zhang, J. H. Lee, K. Brammer, R. Lal, M. Karin and S. Jin, *Nano Lett.*, 2010, **10**, 5088-5092.
5. R. J. Amir, S. Zhong, D. J. Pochan and C. J. Hawker, *J. Am. Chem. Soc.*, 2009, **131**, 13949-13951.
6. D. J. Callahan, W. Liu, X. Li, M. R. Dreher, W. Hassouneh, M. Kim, P. Marszalek and A. Chilkoti, *Nano Lett.*, 2012, **12**, 2165-2170.
7. Y. Wang, M. S. Shim, N. S. Levinson, H.-W. Sung and Y. Xia, *Adv. Funct. Mater.*, 2014, **24**, 4206-4220.
8. E. Leclerc, K. S. Furukawa, F. Miyata, Y. Sakai, T. Ushida and T. Fujii, *Biomaterials*, 2004, **25**, 4683-4690.
9. S. R. MacEwan and A. Chilkoti, *Nano Lett.*, 2014, **14**, 2058-2064.
10. L. M. Randolph, M.-P. Chien and N. C. Gianneschi, *Chem. Sci.*, 2012, **3**, 1363-1380.
11. M. Zelzer, S. J. Todd, A. R. Hirst, T. O. McDonald and R. V. Ulijn, *Biomater. Sci.*, 2013, **1**, 11-39.
12. M.-P. Chien, A. S. Carlini, D. Hu, C. V. Barback, A. M. Rush, D. J. Hall, G. Orr and N. C. Gianneschi, *J. Am. Chem. Soc.*, 2013, **135**, 18710-18713.
13. Q. Hu, P. S. Katti and Z. Gu, *Nanoscale*, 2014, **6**, 12273-12286.
14. K. T. Wiss, O. D. Krishna, P. J. Roth, K. L. Kiick and P. Theato, *Macromolecules*, 2009, **42**, 3860-3863.
15. B. S. Sumerlin, *ACS Macro Lett.*, 2012, **1**, 141-145.
16. Y. Shachaf, M. Gonen-Wadmany and D. Seliktar, *Biomaterials*, 2010, **31**, 2836-2847.
17. J. Montenegro, M. R. Ghadiri and J. R. Granja, *Acc. Chem. Res.*, 2013, **46**, 2955-2965.
18. M. Danial, C. My-Nhi Tran, P. G. Young, S. Perrier and K. A. Jolliffe, *Nat. Commun.*, 2013, **4**.
19. E. Koivunen, B. Wang and E. Ruoslahti, *Nat. Biotechnol.*, 1995, **13**, 265-270.
20. S. Fernandez-Lopez, H.-S. Kim, E. C. Choi, M. Delgado, J. R. Granja, A. Khasanov, K. Kraehenbuehl, G. Long, D. A. Weinberger, K. M. Wilcoxen and M. R. Ghadiri, *Nature*, 2001, **412**, 452-455.
21. S. R. MacEwan and A. Chilkoti, *Peptide Science*, 2010, **94**, 60-77.
22. D. E. Meyer and A. Chilkoti, *Biomacromolecules*, 2002, **3**, 357-367.
23. R. M. Conrad and R. H. Grubbs, *Angew. Chem. Int. Ed.*, 2009, **48**, 8328-8330.
24. W.-B. Zhang, F. Sun, D. A. Tirrell and F. H. Arnold, *J. Am. Chem. Soc.*, 2013, **135**, 13988-13997.
25. A. A. Bogdanov Jr, R. Weissleder, H. W. Frank, A. V. Bogdanova, N. Nossif, B. K. Schaffer, E. Tsai, M. I. Papisov and T. J. Brady, *Radiology*, 1993, **187**, 701-706.
26. M. P. Thompson, L. M. Randolph, C. R. James, A. N. Davalos, M. E. Hahn and N. C. Gianneschi, *Polym. Chem.*, 2014, **5**, 1954-1964.
27. H. Nuhn and H.-A. Klok, *Biomacromolecules*, 2008, **9**, 2755-2763.
28. R. Hourani, C. Zhang, R. van der Weegen, L. Ruiz, C. Li, S. Keten, B. A. Helms and T. Xu, *J. Am. Chem. Soc.*, 2011, **133**, 15296-15299.
29. B. Keil, *Specificity of Proteolysis*, Springer-Verlag Berlin-Heidelberg-New York, 1992.
30. C. W. Bielawski and R. H. Grubbs, *Prog. Polym. Sci.*, 2007, **32**, 1-29.
31. M. S. Sanford, J. A. Love and R. H. Grubbs, *Organometallics*, 2001, **20**, 5314-5318.
32. S. K. Roberts, A. Chilkoti and L. A. Setton, *Biomacromolecules*, 2007, **8**, 2618-2621.
33. D. E. Meyer and A. Chilkoti, *Biomacromolecules*, 2004, **5**, 846-851.
34. F. Fernández-Trillo, A. Duréault, J. P. M. Bayley, J. C. M. van Hest, J. C. Thies, T. Michon, R. Weberskirch and N. R. Cameron, *Macromolecules*, 2007, **40**, 6094-6099.
35. D. Roy, W. L. A. Brooks and B. S. Sumerlin, *Chem. Soc. Rev.*, 2013, **42**, 7214-7243.
36. S. Aluri, M. K. Pastuszka, A. S. Moses and J. A. MacKay, *Biomacromolecules*, 2012, **13**, 2645-2654.
37. Z. Wang, Y. Li, X.-H. Dong, X. Yu, K. Guo, H. Su, K. Yue, C. Wesdemiotis, S. Z. D. Cheng and W.-B. Zhang, *Chem. Sci.*, 2013, **4**, 1345-1352.
38. A. O. Moughton and R. K. O'Reilly, *Chem. Commun.*, 2010, **46**, 1091-1093.
39. Z.-X. Zhang, K. L. Liu and J. Li, *Macromolecules*, 2011, **44**, 1182-1193.
40. N. N. Shahidan, R. Liu, F. Cellesi, C. Alexander, K. M. Shakesheff and B. R. Saunders, *Langmuir*, 2011, **27**, 13868-13878.
41. I. M. Noebauer-Huhmann, P. Szomolanyi, V. Juras, O. Kraff, M. E. Ladd and S. Trattnig, *Invest. Radiol.*, 2010, **45**, 554-558.